Full Paper

Wiley Online Library

ELECTROANALYSIS

DOI: 10.1002/elan.201700247

Ionic Diode Characteristics at a Polymer of Intrinsic Microporosity (PIM) | Nafion "Heterojunction" Deposit on a Microhole Poly(ethylene-terephthalate) Substrate

Budi Riza Putra,[a, b] Barak D.B. Aaronson,[a] Elena Madrid,[a] Klaus Mathwig,[c] Mariolino Carta,[d] Richard Malpass-Evans,[d] Neil B. McKeown,[d] and Frank Marken*[a]

Abstract: Ionic diode phenomena occur at asymmetric ionomer | aqueous electrolyte microhole interfaces. Depending on the applied potential, either an "open" or a "closed" diode state is observed switching between a high ion flow rate and a low ion flow rate. Physically, the "open" state is associated mainly with conductivity towards the microhole within the ionomer layer and the "closed" state is dominated by restricted diffusion-migration access to the microhole interface opposite to the ionomer. In this report we explore a "heterojunction" based on an asymmetric polymer of intrinsic microporosity (PIM) | Nafion ionomer microhole interface. Improved diode characteristics and current rectification are observed in aqueous NaCl. The effects of creating the PIM | Nafion micro-interface are investigated and suggested to lead to novel sensor architectures.

Keywords: Ionomer · polymer interface · voltammetry · nanofluidics · ionic diode · desalination

1 Introduction

Ionic diode (or current rectification) effects are observed in several types of eletrolytic systems including nanopores [1] and nanocones [2], asymmetric solution membrane devices [3,4], microchannels with ionomer deposits [5,6], and hydrogel interfaces [7,8], where ion depletion and accumulation phenomena are possible. We have recently observed current rectification for asymmetric ionomer deposits on microhole substrates for Nafion [9], for cellulose [10], and for polymers of intrinsic microporosity [11,12]. Potential applications envisaged for these ionic diode devices are in desalination [13], energy harvesting [14], in "iontronics" [15], as well as potentially in electroanalysis, if diodes can be made more selective to target specific ions [16]. Providing a microporous coating opposite to the ionomer (Nafion) layer in ionic diodes could provide a way to improve selectivity and to define and active sensor interface.

Polymers of intrinsic microporosity (PIMs) provide a novel and versatile class of materials [17,18]. Generally, PIMs are based on highly rigid molecular polymer structures that pack space poorly and therefore provide solid films with high internal porosity and surface area [19], which can be exploited in gas adsorption [20] and separation [21]. Further benefits from the molecularly rigid structure are good solubility in certain organic solvents (e.g. chloroform), and therefore good processibility [22], thermal stability [23], and retention of porosity even under carbonisation conditions [24]. Both the carbonised and the parent form of the microporous material have been employed as nano-particle electrocatalyst substrate [25,26].

Electrochemical applications of PIMs have been suggested in fuel cell catalysis [27], in heterogenisation of catalysts [28], and in highly ion-conductive [29] and ion-selective membranes [30]. PIMs deposited asymmetrically onto a 20 μm diameter microhole in a poly-ethylene-terephthalate (PET) film have been shown to give rise to ionic diode behaviour, but also demonstrate "ionic flip-flop" characteristics when exposed to phytate anions [31]. For the PIM-EA-TB material (see structure in Figure 1; PIM = polymer of intrinsic microporosity; EA = ethano-anthracene; TB=Tröger base) current rectification effects have been observed as a function of pH. At approximately pH 4 protonation of the tertiary amine was found to convert the neutral PIM-EA-TB structure into an anion conducting structure [31]. Therefore, PIM-EA-TB can be considered predominantly neutral and both Na^+ and Cl^- conducting when immersed in neutral aqueous NaCl, but

[a] B. R. Putra, B. D. Aaronson, E. Madrid, F. Marken
Department of Chemistry, University of Bath, Claverton Down, BA2 7AY, UK
E-mail: f.marken@bath.ac.uk
[b] B. R. Putra
Department of Chemistry, Faculty of Mathematics and Natural Sciences, Bogor Agricultural University, Bogor, West Java, Indonesia
[c] K. Mathwig
Groningen Research Institute of Pharmacy, Pharmaceutical Analysis, University of Groningen, P.O. Box 196, 9700 AD Groningen, The Netherlands
[d] M. Carta, R. Malpass-Evans, N. B. McKeown
School of Chemistry, University of Edinburgh, Joseph Black Building, West Mains Road, Edinburgh, Scotland EH9 3JJ, UK

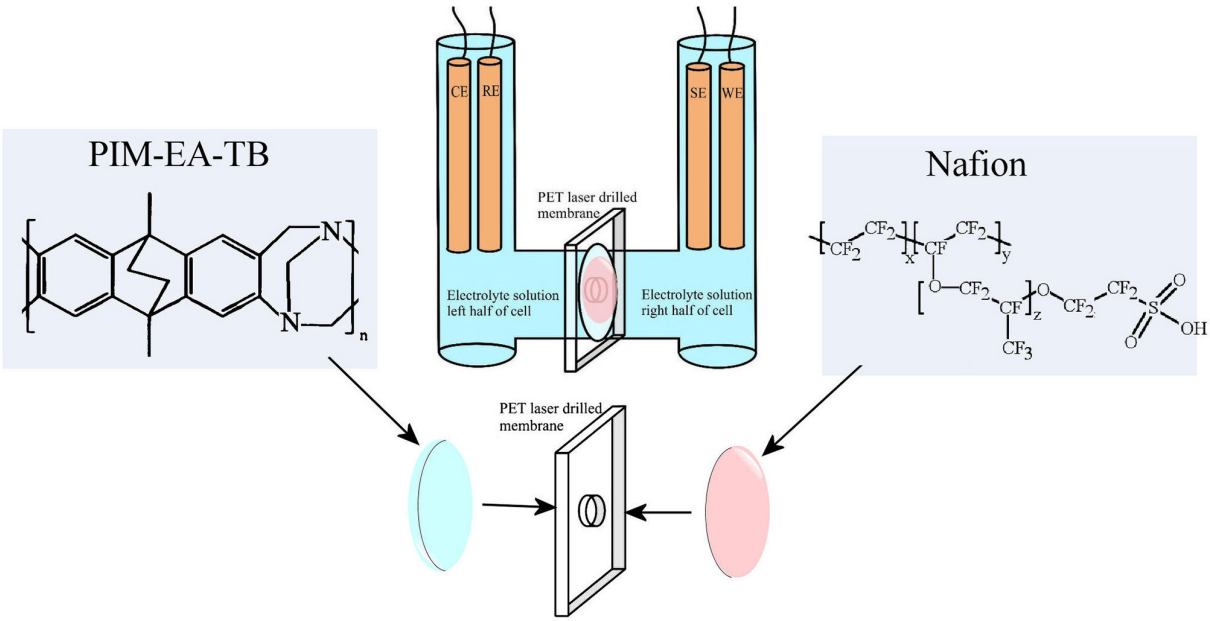

Fig. 1. Schematic drawing of the experimental 4-electrode system with a PET film separating two half-cells. The laser-drilled microhole of approximately 20 μm diameter is covered with deposits of PIM-EA-TB and Nafion (see molecular structures).

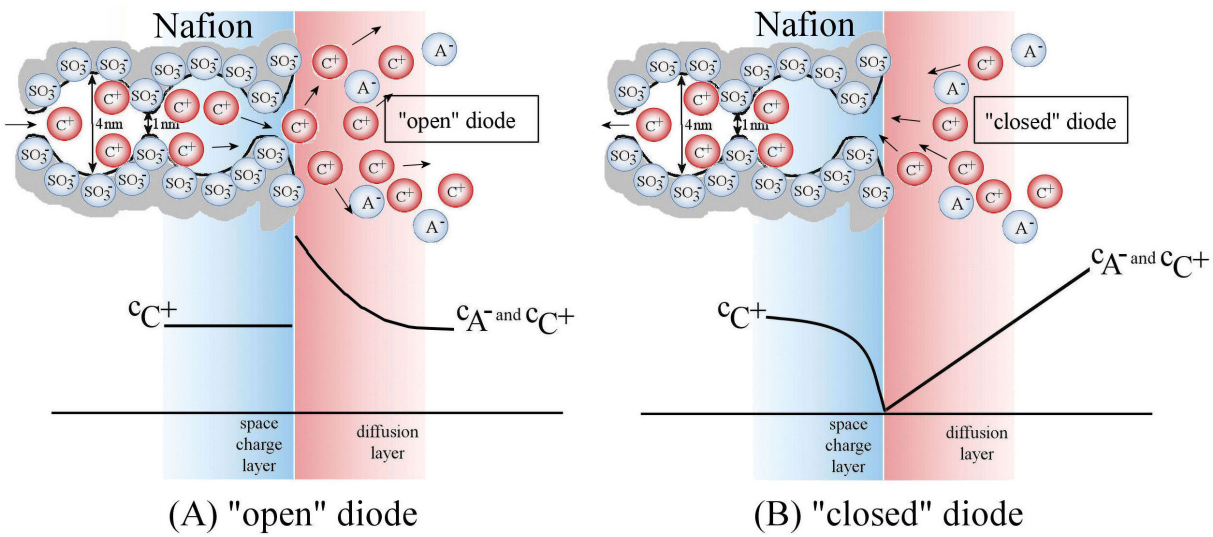

Fig. 2. Schematic drawing of ion transport conditions at a Nafion | aqueous electrolyte micro-interface for (A) the "open" diode and (B) the "closed" diode. In (A) the transport of cations is impeded primarily by resistance in the Nafion ionomer, whilst salt concentration can build up in the aqueous side. In (B) the transport is impeded primarily in the aqueous phase by diffusion-migration access to the Nafion ionomer.

predominantly positive (protonated) and probably exclusively Cl^- conducting when immersed into aqueous HCl.

Commercial Nafion ionomer, when deposited onto a 20 μm diameter microhole in a PET film (see Figure 1 was found to provide effective current rectification effects not only for acidic environments, but also for neutral solutions of NaCl or KCl [9]. The cation conduction through Nafion was observed to be uni-directional due to the asymmetric geometry of the deposit on the PET substrate. The mechanism behind the current rectification process for Nafion has been reported to be based mainly on two cases: (A) the "open" diode, where cations access the microhole via Nafion with a resulting high conductivity and some accumulation of salt in the adjacent solution phase; (B) the "closed" diode where cations access the microhole from the opposite solution phase, where lower conductivity leads to mass transport limitation and concentration polarisation. Figure 2 shows a schematic drawing of the two situations.

In this report, the Nafion deposit on the microhole in PET is complemented by an opposite PIM-EA-TB deposit (see Figure 1) to replace the aqueous electrolyte phase. This constitutes a new type of "heterojunction" with ionic diode characteristics that are dependent on both materials as well as the aqueous solution environment. It is demonstrated that both the "closed" and the "open" diode can be affected by the PIM-EA-TB film. Improved diode characteristics and rectification are observed. The focus here is on cationic diode applications (potentially for desalination) in aqueous NaCl solution, but (in future) this heterojunction prototype could be configured also as "anionic diode" or to provide more ion selective diodes for analytical applications. Importantly, the PIM | Nafion interface defines a new reaction zone in which "sensing processes" can be confined to lead to high amplificaiton effects, for example when analyte causes localised switching of the state of the diode form closed to open. In future, further applications of ionic heterojunction diodes in sensing are expected.

2 Experimental

2.1 Chemical Reagents

Nafion®–117 (5% in a mixture of lower aliphatic alcohol and water), concentrated hydrochloric acid (37%), sodium chloride, rhodamine B (97%), and eosin Y were obtained from Sigma-Aldrich or Fisher Scientific and used without further purification. Solutions were prepared under ambient conditions in volumetric flasks with ultrapure water of resistivity 18.2 MΩ cm from ELGA Purelab Classic system.

2.2 Instrumentation

Electrochemical data (for both voltammetry and chronoamperometry) were recorded at $T = 20 \pm 2$ °C on a potentiostat system (Ivium Compactstat, Netherlands). A classic 4-electrode electrochemical cell similar to that employed in previous membrane conductivity studies was used. The membrane separates two tubular half-cells (15 mm diameter, see Figure 1), one with Pt wire working and saturated calomel (SCE) sense electrode and the other with SCE reference electrode and Pt wire counter electrode. In electrochemical measurements the working electrode was always located on the side of Nafion films. Fluorescence imaging experiments were performed on a Carl Zeiss Confocal Scanning Microscpore. For fluorescence analysis, rhodamine B was mixed with Nafion-117 solution and eosin-Y was mixed with PIM-EA-TB (2% in chloroform), which were then applied to opposite sides of the PET films (see below).

2.3 Procedure

In order to form films of Nafion and PIM-EA-TB on PET substrates (obtained with 20 μm diameter hole in 6 μm thick PET from Laser-Micro-Machining Ltd., Birmingham, UK) a two-step solution casting method was employed. The PET film was placed on a glass substrate (pre-coated with a thin layer of 1% agarose gel by solution-casting). A volume of 10 μL PIM-EA-TB solution (2% in chloroform) was applied to the surface and with a glass rod the PIM-EA-TB solution was spread evenly over the PET to give a 1 cm^2 film, which after drying produced a thin uniform coating typically 10 μm thickness (by fluorecence imaging). Next, the PET film was turned around and coated with a volume of 10 μL Nafion solution from the opposite side. In order to image the Nafion and PIM-EA-TB film fluorescence image stacks were obtained. Figure 3 shows a typical image stack with red coloration indicating rhodamine B in Nafion and yellow coloration indicating eosin Y in PIM-EA-TB. Although partially obscured by shadowing effects, three layers can be seen corresponding to Nafion (ca. 6 μm thick), PET (ca. 6 μm thick), and PIM-EA-TB (ca. 10 μm thick).

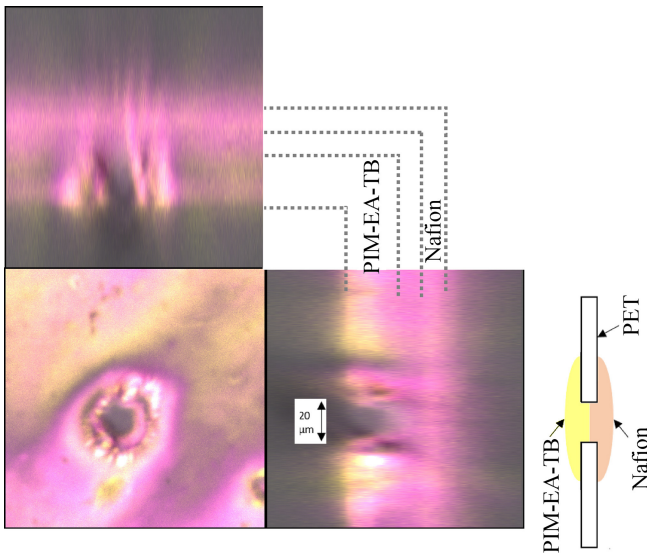

Fig. 3. Fluorescence micrograph (coloration red associated with rhodamine B and yellow with eosin Y) showing the cross-section and the top view (central slice) for a PIM-EA-TB | Nafion heterojunction. Nafion was stained with rhodamine B and PIM-EA-TB was stained with eosin Y.

3 Results and Discussion

3.1 Ionic Rectification Effects as a Function of NaCl or HCl Concentration: Symmetric

It has been reported previously that Nafion when deposited onto a microhole (20 μm diameter) in a poly-(ethylene-terephthalate) film (PET, 6 μm thick) causes effective ionic current rectification [9]. The rectification ratio (obtained by dividing the current at +1 V by the current at −1 V) was reported to be typically 10 – 20 for both aqueous HCl and aqueous NaCl. The rectification ratio decreased significantly when the concentration of

aqueous electrolyte was increased on the side opposite to the Nafion deposit, but not when the aqueous electrolyte concentration was increased on the Nafion side. The reason for this behaviour can be traced back to the diode mechanism, which suggests that the current for the open diode is dependent on transport of cations through Nafion (from the side of the Nafion deposit) and the current for the closed diode is dependent on the transport of cations in the aqueous phase close to the microhole. For applications of the ionic diode a high rectification effect (low resistivity when open, high resistivity when closed, and fast switching speed) is desirable.

When depositing a film of PIM-EA-TB (see structure in Figure 1) on the opposite side to Nafion onto the 20 μm diameter microhole, a new type of interface is created. Figure 4 A shows cyclic voltammetry data for this PIM-EA-TB | Nafion heterojunction immersed in aqueous NaCl for 1 mM, 10 mM, and 100 mM solution on both sides of the dual-material membrane. Voltammetric data are recorded over a +/−4 V potential range. With concentration of NaCl the rectification ratio is significantly increased. The magnitude of currents also seems to be slightly higher compared to that reported for Nafion

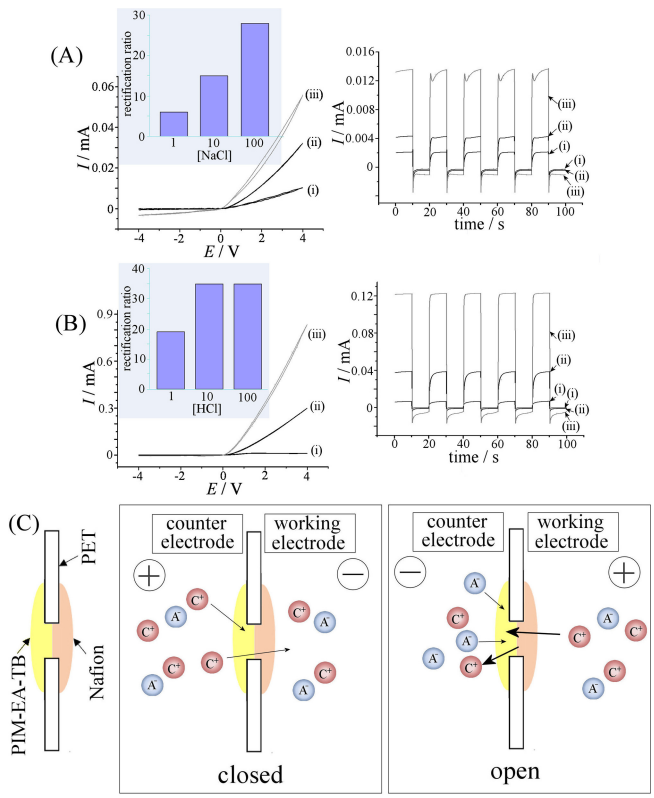

Fig. 4. (A) Cyclic voltammograms (scan rate 25 mVs^{-1}) and chronoamperometry data (stepping from +1 V to −1 V) for a PIM-EA-TB | Nafion heterojunction immersed in aqueous NaCl (1, 10, 100 mM) on both sides. Inset: rectification ratio at +/1 V. (B) As above, but for aqueous HCl. (C) Schematic drawing of ion flow in closed and open diode states (see text).

only [9]. Both are useful observations for ionic diode optimisation.

Next, the experiment is repeated with aqueous HCl. With Nafion only, aqueous HCl generally caused a higher current for the open diode [9] due to the higher mobility of protons. Here, clearly the currents for both open and closed diodes are higher (almost approaching 1 mA in the open state). At the same time the rectification ratio is improved (roughly doubled). Most intriguing is the result for the 1 mM HCl solution, where a new limiting current is observed stabilising at potentials positive of approximately 1 V (see Figure 4 Bi). This phenomenon can be explained when considering the ion flow for closed and open diode states (Figure 4C). The overall behaviour of the diode is dominated by the Nafion layer only allowing cation transport. In the closed state (at negative applied potentials) cations have to enter via the PIM-EA-TB to then conduct through the Nafion. In the absence of the PIM-EA-TB layer, diffusion-migration in the aqueous phase would limit the transport [9]. In the presence of PIM-EA-TB and at a pH > 4 the polymer is predominantly uncharged [31] and only some NaCl will enter the microporous film to conduct. The current is lower than that seen in the absence of PIM-EA-TB. In the presence of PIM-EA-TB and at pH < 4 the polymer is protonated and mainly anion-conducting (due to very low mobility of protons attached to the PIM-EA-TB backbone). However, it remains poorly cation/proton conducting and this causes a low current in the closed state (Figure 4 Bi).

In the open state, a similar argument applies and flow of cations is fast across both the Nafion and the PIM-EA-TB layer. At pH > 4 additional chloride can enter the PIM-EA-TB to increase conductivity. At a pH < 4 cation conductivity is poor and for 1 mM HCl a new limiting current (positive of +1 V) shows that PIM-EA-TB blocks the current even when Nafion is highly conducting under these conditions. Both Nafion and PIM-EA-TB layers operate synergistically to provide an improved or modified ionic diode effect.

3.2 Ionic Rectification Effects as a Function of NaCl or HCl Concentration: Asymmetric

When placing the PIM-EA-TB | Nafion heterojunction between 10 mM HCl and 10 mM NaCl, new effects are observed. Figure 5 A demonstrates that generally currents are lower and a limiting current in the open diode state is observed at elevated scan rates (higher than 100 mVs^{-1}). This effect is consistent with that observed in Figure 4B when the PIM-EA-TB film is exposed to acidic solution. The current that passes through the protonated PIM-EA-TB is limited by cation (sodium) mobility. At slower scan rates the PIM-EA-TB is likely to be deprotonated to allow Na^+ to pass (below a scan rate of 100 mVs^{-1}).

When switching sides with 10 mM HCl contacting Nafion and 10 mM NaCl containing PIM-EA-TB, normal diode characteristics (see Figure 5B) are restored, however, currents are decreased when compared to the

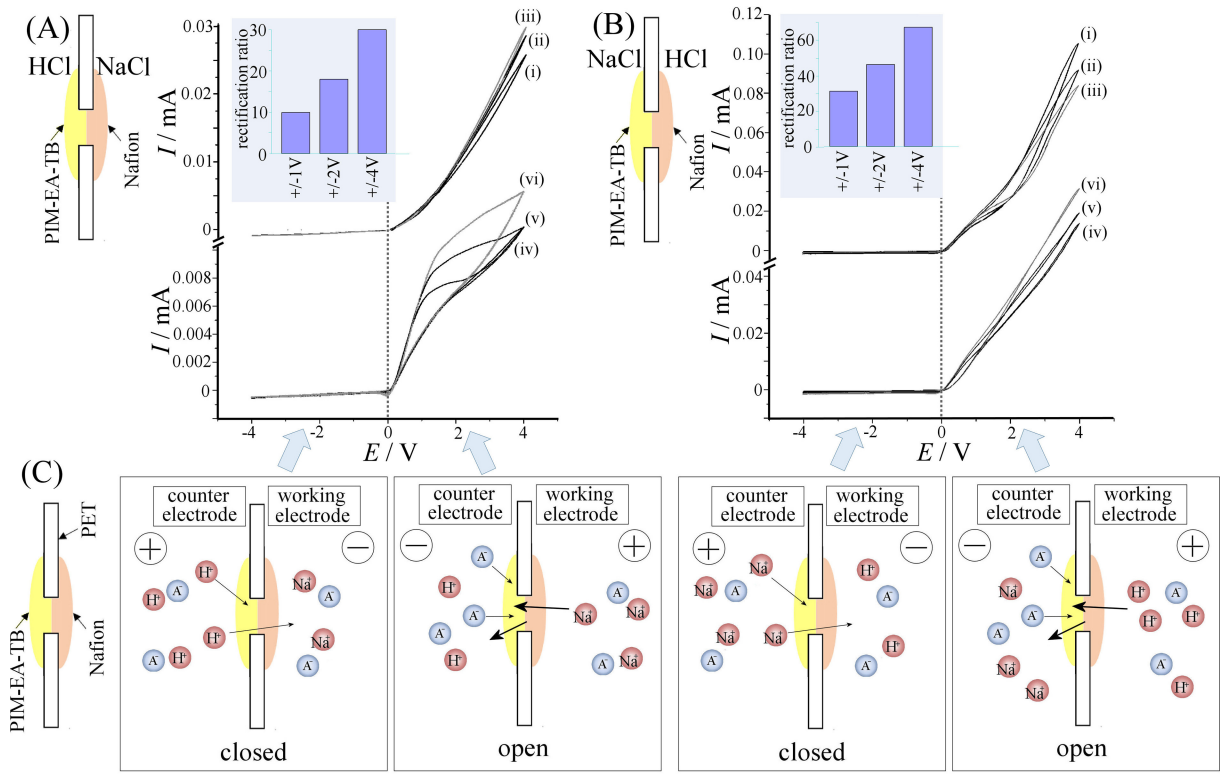

Fig. 5. (A) Cyclic voltammograms (scan rate (i) 25, (ii) 50, (iii) 100, (iv) 250, (v) 500, (vi) 1000 mVs^{-1}) for a PIM-EA-TB | Nafion heterojunction immersed in 10 mM HCl–10 mM NaCl. (B) As before, but for 10 mM NaCl10 mM HCl. (C) Schematic drawings explaining the four cases of open and closed diode behaviour.

10 mM HCl–10 mM HCl case (see Figure 4B). Figure 5C summarises the observed effects schematically. Data in Figure 5 A can be considered consistent with a "sodium diode" whereas data in Figure 5B suggest a "proton diode".

When inspecting the cyclic voltammogram in Figure 5 A at a high scan rate of 1000 mVs^{-1}, it is possible to see a small cathodic peak emerging at approximately 0 V. This peak is associated with the switching time of the heterojunction diode for the case of switching from open state to closed state. In the open state sodium cations flow through the Nafion and then through the PIM-EA-TB side possibly pushing protons out. Upon switching the diode to closed state, the protons have to re-enter the film, which leaves a short period of current flow (due sodium cation removal and protons re-entering the PIM-EA-TB layer). Further details can be observed when investigating chronoamperometry current data.

3.3 Ionic Rectification Effects as a Function of Time

When investigating the chronoamperometry data (see Figure 4B) for the HCl–HCl case, a cathodic current spike upon closing and a rising anodic transient upon diode opening are observed. Both can be explained with the build-up and decline in proton concentration in the PIM-EA-TB layer. For the NaCl–NaCl experiment (Figure 4 A) a more complex two-component transient is observed. Both diode opening and closing appear to be associated with an initial fast spike followed by another slower rise in anodic or cathodic current, respectively. This may be associated with fast anion transport followed by slower accumulation of both sodium and chloride to fully develop the concentration profile across the two polymer materials.

Figure 6 A shows data for the case of a fixed 100 mM NaCl concentration in contact with PIM-EA-TB and a variable concentration of NaCl in contact with Nafion. The increase in the NaCl concentration clearly improves the rectification ratio mainly due to a higher conductivity across the Nafion layer (with currents approaching 1 mA through a 20 µm diameter microhole). When increasing the NaCl concentration on the PIM-EA-TB side (Figure 5B) the opposite behaviour is observed with a strong loss of rectification effect. An increase in NaCl in this case is likely to also increase the salt content in the PIM-EA-TB porous strucutre, which is detrimental in the closed state of the diode. It can be concluded that both materials Nafion and PIM-EA-TB perform distinct tasks in the ionic diode. Nafion is receiving the charge carriers (here Na^+) and requires high conductivity and PIM-EA-TB blocks the return of charge carriers, which is affected by the type and concentration of electrolyte in contact to the PIM-EA-TB deposit.

It is insightful to explore the conditions for good rectification effects to be observed for "sodium diodes".

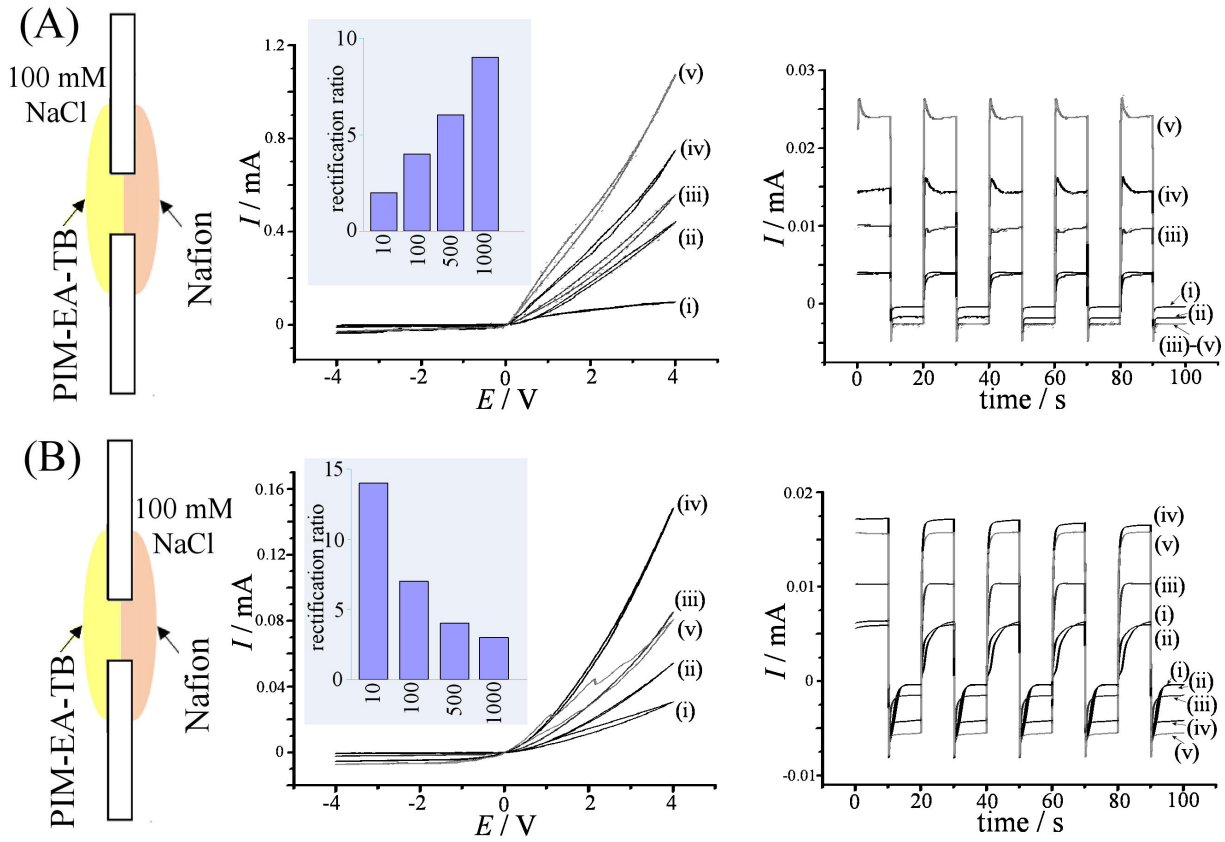

Fig. 6. (A) Cyclic voltammetry data (scan rate 25 mVs^{-1}) for a PIM-EA-TB | Nafion heterojunction with 100 mM NaCl in contact to PIM-EA-TB and (i) 1, (ii) 10, (iii) 100, (iv) 500, (v) 1000 mM NaCl in contact to Nafion. Also shown chronoamperometry data for +1 V to −1 V transients. (B) As above but 100 mM NaCl in contact to Nafion and (i) 1, (ii) 10, (iii) 100, (iv) 500, (v) 1000 mM NaCl in contact to PIM-EA-TB.

A high concentration of NaCl on the Nafion side as well as a low concentration of NaCl on the PIM-EA-TB side are beneficial. Protonation of PIM-EA-TB appears to be detrimental (see Figure 5 A). A wider range of cation and anion "interference" effects (beyond protons) may be possible and needs to be further investigated. For practical applications of these ionic diode systems (for example in desalination) the rectification ratio will need to be further improved and an appropriate pair of anionic diode and cationic diode will be required. For the case of the heterojunction, PIM-EA-TB or similar PIM materials could be employed in both cases to modify diode characteristics or to better control processes within the microhole. For the development of novel sensor diodes changes in surface charge in the PIM material or at the PIM | Nafion interface could be employed to modulate the open state or closed state ion currents, for example based on analyte binding to surface functional groups.

4 Conclusions

It has been demonstrated that "heterojunctions" are readily fabricated by deposition of Nafion onto one side of a 20 μm diameter microhole in PET and deposition of PIM-EA-TB on the opposite side. The presence of the PIM-EA-TB affects access of cations and anions to the PIM | Nafion interface and it helps defining an interface where processes such as salt precipitation could occur.

Further work will be necessary to explore effects of film thickness for both Nafion and for PIM-EA-TB. The effects of solution composition have been shown for NaCl and HCl, but a much wider range of cations and anions will be of interest. Improved ionomer selectivity on both sides of the heterojunction could be used to develop ionic diodes for example for K^+, Mg^{2+}, Ca^{2+}, and/or more complex cations and anions. Also, a broader range of PIMs and ionomers could be investigated to further optimize ionic diode performance. Last-but-not-least, it will be necessary to develop computational models with predictive power to screen a wider parameter space and to predict new electrolytic device configurations.

Acknowledgements

B.R.P. thanks to Indonesian Endowment (LPDP RI) for a PhD scholarship. B.D.B.A. is grateful for support from the Leverhulme Foundation (RPG-2014-308: "New Materials for Ionic Diodes and Ionic Photodiodes"). E.M. and F.M.

acknowledge financial support from the EPSRC (EP/K004956/1).

References

[1] W. J. Lan, M. A. Edwards, L. Luo, R. T. Perera, X. J. Wu, C. R. Martin, H. S. White, *Acc. Chem. Res.* **2016**, *49*, 2605–2613.
[2] H. C. Zhang, Y. Tian, L. Jiang, *Nano Today* **2016**, *11*, 61–81.
[3] R. Zhao, G. H. He, Y. L. Deng, *Electrochem. Commun.* **2012**, *23*, 106–109.
[4] E. Madrid, M. A. Buckingham, J. M. Stone, A. T. Rogers, W. J. Gee, A. D. Burrows, P. R. Raithby, V. Celorrio, D. J. Fermin, F. Marken, *Chem. Commun.* **2016**, *52*, 2792–2794.
[5] Y. Green, Y. Edri, G. Yossifon, *Phys. Rev. E* **2015**, *92*, 033018.
[6] G. C. Sun, S. Senapati, H. C. Chang, *Lab-on-a-chip* **2016**, *16*, 1171–1177.
[7] B. Lovrecek, A. Despic, J. O. M. Bockris, *J. Phys. Chem.* **1959**, *63*, 750–751.
[8] L. Hegedus, N. Kirschner, M. Wittmann, Z. Noszticzius, *J. Phys. Chem. A* **1998**, *102*, 6491–6497.
[9] D. P. He, E. Madrid, B. D. B. Aaronson, L. Fan, J. Doughty, K. Mathwig, A. M. Bond, N. B. McKeown, F. Marken, *ACS Appl. Mater. Interf.* **2017**, *9*, 11272–11278.
[10] B. D. B. Aaronson, D. P. He, E. Madrid, M. A. Johns, J. L. Scott, L. Fan, J. Doughty, M. A. S. Kadowaki, I. Polikarpov, N. B. McKeown, F. Marken, *ChemSelect* **2017**, *2*, 871–875.
[11] Y. Y. Rong, Q. L. Song, K. Mathwig, E. Madrid, D. P. He, R. G. Niemann, P. J. Cameron, S. E. C. Dale, S. Bending, M. Carta, R. Malpass-Evans, N. B. McKeown, F. Marken, *Electrochem. Commun.* **2016**, *69*, 41–45.
[12] Y. Y. Rong, A. Kolodziej, E. Madrid, M. Carta, R. Malpass-Evans, N. B. McKeown, F. Marken, *J. Electroanal. Chem.* **2016**, *779*, 241–249.
[13] E. Madrid, P. Cottis, Y. Y. Rong, A. T. Rogers, J. M. Stone, R. Malpass-Evans, M. Carta, N. B. McKeown, F. Marken, *J. Mater. Chem. A* **2015**, *3*, 15849–15853.
[14] S. Tseng, Y. M. Li, C. Y. Lin, J. P. Hsu, *Nanoscale* **2016**, *8*, 2350–2357.
[15] H. G. Chun, T. D. Chung, in R. G. Cooks, J. E. Pemberton, eds., Annual Review of Analytical Chemistry (2015) Vol. 8, pp. 441–462.
[16] E. B. Kalman, O. Sudre, I. Vlassiouk, Z. S. Siwy, *Anal. Bioanal. Chem.* **2009**, *394*,413–419.
[17] N. B. McKeown, P. M. Budd, *Macromolecules* **2010**, *43*, 5163–5176.
[18] N. B. McKeown, P. M. Budd, *Chem. Soc. Rev.* **2006**, *35*, 675–683.
[19] M. Carta, R. Malpass-Evans, M. Croad, Y. Rogan, J. C. Jansen, P. Bernardo, F. Bazzarelli, N. B. McKeown, *Science* **2013**, *339*, 303–307.
[20] B. S. Ghanem, M. Hashem, K. D. M. Harris, K. J. Msayib, M. C. Xu, P. M. Budd, N. Chaukura, D. Book, S. Tedds, A. Walton, N. B. McKeown, *Macromolecules* **2010**, *43*, 5287–5294.
[21] Y. C. Xiao, L. L. Zhang, L. Xu, T. S. Chung, *J. Membrane Sci.* **2017**, *521*, 65–72.
[22] P. M. Budd, B. S. Ghanem, S. Makhseed, N. B. McKeown, K. J. Msayib, C. E. Tattershall, *Chem. Commun.* **2004**, 230–231.
[23] F. Y. Li, Y. C. Xiao, T. S. Chung, S. Kawi, *Macromolecules* **2012**, *45*, 1427–1437.
[24] Y. Y. Rong, D. P. He, A. Sanchez-Fernandez, C. Evans, K. J. Edler, R. Malpass-Evans, M. Carta, N. B. McKeown, T. J. Clarke, S. H. Taylor, A. J. Wain, J. M. Mitchels, F. Marken, *Langmuir* **2015**, *31*, 12300–12306.
[25] Y. Y. Rong, D. P. He, R. Malpass-Evans, M. Carta, N. B. McKeown, M. F. Gromboni, L. H. Mascaro, G. W. Nelson, J. S. Foord, P. Holdway, S. E. C. Dale, S. Bending, F. Marken, *Electrocatalysis* **2017**, *8*, 132–137.
[26] D. P. He, D. S. He, J. L. Yang, Z. X. Low, R. Malpass-Evans, M. Carta, N. B. McKeown, F. Marken, *ACS Appl. Mater. Interf.* **2016**, *8*, 22425–22430.
[27] D. P. He, Y. Y. Rong, M. Carta, R. Malpass-Evans, N. B. McKeown, F. Marken, *RSC Adv.* **2016**, *6*, 9315–9319.
[28] S. D. Ahn, A. Kolodziej, R. Malpass-Evans, M. Carta, N. B. McKeown, S. D. Bull, A. Buchard, F. Marken, *Electrocatalysis* **2016**, *7*, 70–78.
[29] Z. J. Yang, R. Guo, R. Malpass-Evans, M. Carta, N. B. McKeown, M. D. Guiver, L. Wu, T. W. Xu, *Angew. Chem. Internat. Ed.* **2016**, *55*, 11499–11502.
[30] I. Chae, T. Luo, G. H. Moon, W. Ogieglo, Y. S. Kang, M. Wessling, *Adv. Energy Mater.* **2016**, *6*, 1600517.
[31] E. Madrid, Y. Y. Rong, M. Carta, N. B. McKeown, R. Malpass-Evans, G. A. Attard, T. J. Clarke, S. H. Taylor, Y. T. Long, F. Marken, *Angew. Chem. Internat. Ed.* **2014**, *53*, 10751–10754.

Received: April 29, 2017
Accepted: June 16, 2017
Published online on June 27, 2017

